

Effects of the restoration mortar on chalk stone buildings

This content has been downloaded from IOPscience. Please scroll down to see the full text.

2016 IOP Conf. Ser.: Mater. Sci. Eng. 133 012038

(<http://iopscience.iop.org/1757-899X/133/1/012038>)

View [the table of contents for this issue](#), or go to the [journal homepage](#) for more

Download details:

IP Address: 86.127.243.73

This content was downloaded on 04/12/2016 at 09:52

Please note that [terms and conditions apply](#).

Effects of the restoration mortar on chalk stone buildings

R M Ion^{a,b, 1}, S Teodorescu^c, R M Știrbescu^c, I D Dulamă^c, I R Șuică-Bunghiez^b,
I A Bucurică^c, R C Fierăscu^b, I Fierscu^b, M L Ion^d

^aValahia University, Materials Engineering Department, 13 Aleea Sinaia, Targoviste, Romania.

^bICECHIM, 202 Splaiul Independentei, Bucharest-060021, Romania.

^cMultidisciplinary Scientific and Technologic Research Institute, 13 Aleea Sinaia, Targoviste, Romania.

^dValahia University of Targoviste, History Department, 13 Aleea Sinaia, Targoviste, Romania.

E-mail: rodica_ion2000@yahoo.co.uk

Abstract. The monument buildings as components of cultural heritage are exposed to degradation of surfaces and chemical and mechanical degradation, often associated to soiling and irreversible deterioration of the building. In many conservative and restorative works, a cement-based mortar was used without knowing all the adverse effects of this material on the building. This paper deals with the study of the effects of natural cement used in restorative works in the particular case of the Basarabi-Murfatlar Churches Ensemble. Cement-based materials exposed to sulfate present in the chalk stone - gypsum ($\text{CaSO}_4 \cdot 2\text{H}_2\text{O}$), can induce signs of deterioration, due to ettringite ($[\text{Ca}_3\text{Al}(\text{OH})_6 \cdot 12\text{H}_2\text{O}]_2 \cdot (\text{SO}_4)_3 \cdot 2\text{H}_2\text{O}$) or thaumasite ($\text{Ca}_3[\text{Si}(\text{OH})_6 \cdot 12\text{H}_2\text{O}] \cdot (\text{CO}_3) \cdot \text{SO}_4$) formation. These phases contribute to strain within the material, inducing expansion, strength loss, spalling and severe degradation. Several combined techniques (XRD, EDXRF, ICP-AES, SEM, EDS, sulphates content, FT-IR and Raman analysis) were carried out to put into evidence the effects of them on the building walls.

1. Introduction

For understanding deterioration and conservation of stone, especially those from architectural buildings heritage is absolutely necessary to know the structural, chemical and mineralogical composition of the rock and the mechanisms of stone degradation due to the external factors [1].

Carbonate rocks have been widely used as building stones since ancient times, because they are soft, easy to process and cut, mainly due to their composition: various amounts of matrix, biogenic and nonbiogenic components. But, the most important negative aspect of these stones are their damages susceptibility, generally due to the increasing atmospheric pollution by acidic agents [2,3]. Also, the carbonate rocks are characterized by various porosity and water absorption that affect their resistance to frost and salt-crystallization damage [4,5].

Limestone is known as a sedimentary carbonate rock, fine-grained and massive, without visible pores and lack of distinct bedding. Many of limestone buildings have been restored with concrete

¹ To whom any correspondence should be addressed.



mortars, and because after a short time after restoration they show visible damages, is imperious necessary to find the causes responsible for such processes.

Concrete, is a versatile and robust building material, but due to its porosity is susceptible to potentially harmful agents, such as chlorides, sulphates, carbon dioxide, and other pollutants that determine the high decay rate and deterioration of concrete [6]. It has been used in many conservative and restorative works, mostly as cement-based material, but without knowing all the adverse effects of this material on the building. Cement-based materials exposed to sulfate present in the carbonate stones (limestone) as gypsum ($\text{CaSO}_4 \cdot 2\text{H}_2\text{O}$), can induce signs of deterioration, due to ettringite ($[\text{Ca}_3\text{Al}(\text{OH})_6 \cdot 12\text{H}_2\text{O}]_2 \cdot (\text{SO}_4)_3 \cdot 2\text{H}_2\text{O}$) or thaumasite ($\text{Ca}_3[\text{Si}(\text{OH})_6 \cdot 12\text{H}_2\text{O}] \cdot (\text{CO}_3) \cdot \text{SO}_4$) presence. These newly solid phases can lead to strain within the material, inducing expansion, strength loss, spalling and severe degradation of the wall building [7-9].

Our study aimed to determine the influence in time of the cement-based mortars used to restoration procedures, and to show how these mortars are a continuous source for a deterioration process for the building walls, due to thaumasite and ettringite formation. As a particular case, will be evaluated the effects of these cement-based mortars used in restorative works in the Basarabi-Murfatlar Churches Ensemble. Several analytic techniques (XRD, EDXRF, ICP-AES, SEM, sulphates content, FT-IR and Raman analysis) were carried out to put into evidence the effects of degradation on the building walls.

2. Materials and methods

As materials, has been used a small piece of chalk (B4) and a small piece of restoration mortar (BMR) both of them detached from the church and without patrimonial value.

X-ray diffraction analyses were performed using a Rigaku SmartLab equipment, operating at 45 kV and 200 mA, using $\text{Cu K}\alpha$ radiation (1.54059 \AA), in parallel beam configuration, from 3 to 90 2θ degrees; the components were identified using the Rigaku Data Analysis Software PDXL 2 and available literature data.

The X-ray fluorescence was used to identify the elements in certain pigments, fillers. The determinations were carried out using an energy-dispersive spectrometer, EDXRF PW4025, Minipal 2 - PANalytical, with a Si-PIN detector.

Trace elements were quantified using **ICP-AES** (inductively coupled plasma-atomic emission) spectrometer Varian Liberty 110 Series. The samples were cut off from the original shreds and were finely powdered in an agate mortar. Multielement, matrix matched standards were used for the quantitative determinations. Microwave assisted digestions were performed in a Berghof microwave oven with the use of high-pressure closed Teflon PFA vessels and online pressure and temperature control.

Raman spectra have been obtained with a portable dual wavelength Raman analyzer IR - XANTUS 2 -RIGAKU, with the following parameters: Dual wavelength source 1064nm & 785nm, spectral range (cm^{-1}) 200 – 4000, Spectral Resolution (cm^{-1}) 7 – 10, Laser Output Power (mW) 400 – 490, Laser Output Power (mW) 30 – 490, cooled detectors – CCD and InGaAs. The paint cross sections were analyzed using Raman spectroscopy in order to identify pigments and fillers. The laser beam was focused on a diameter of about 25, 5 and 1.5–2 μm , respectively. Spectra were acquired using 10 s of signal collection time and five accumulations.

Light Optical Microscopy (LOM) has been recorded by using NOVEX microscope with a Leica EC3 camera under a magnification of 40x to 600x, to determine the matrix heterogeneity, particle size, color, shape and transparency.

Scanning electron microscopy (SEM) has been achieved with a SU-70 (manufacturer Hitachi, Japan) COUPLED ENERGY dispersive spectrometer (EDS) spectrometer wavelength dispersive (WDS). SEM magnification range of 30X-800.000X and the resolution accelerating voltage of 15 KV is 1 nm. The spectrometer EDS attached allows qualitative and quantitative analysis (from Be ($Z = 4$) to Pu ($Z = 94$)) on point, rectangle, circle or the freedom of choice, analysis and line type grid mapping X-ray solutions for overlapping peaks. WDS spectrometer attached allows qualitative and quantitative analysis (B ($Z = 5$) to Pu ($Z = 94$)).

The sulphates attack tests carried out on brushed samples were made according to the SR EN ISO 787-13:2003 “General methods of test for pigments Part 13: Determination of water soluble sulphates, chlorides and nitrates” and SR EN ISO 787-8:2003: “General methods of test for pigments and extenders – Part 8: Determination of matter soluble in water – Cold extraction method”.

3. Results and discussions

As a first step of the samples identification procedures, the two samples were subjected to X-ray fluorescence analysis (figure 1). The two samples are dominated by calcium [10]. The main difference regarding the trace elements composition is the presence of aluminium and iron in higher amount in the wall filler than in the wall itself. Those results are confirmed by the ICP-AES analyses: for the wall samples, 350 ppm Al, and, respectively, 242 ppm Fe; for the wall filler samples, 575 ppm Al, and, respectively, 358 ppm Fe.

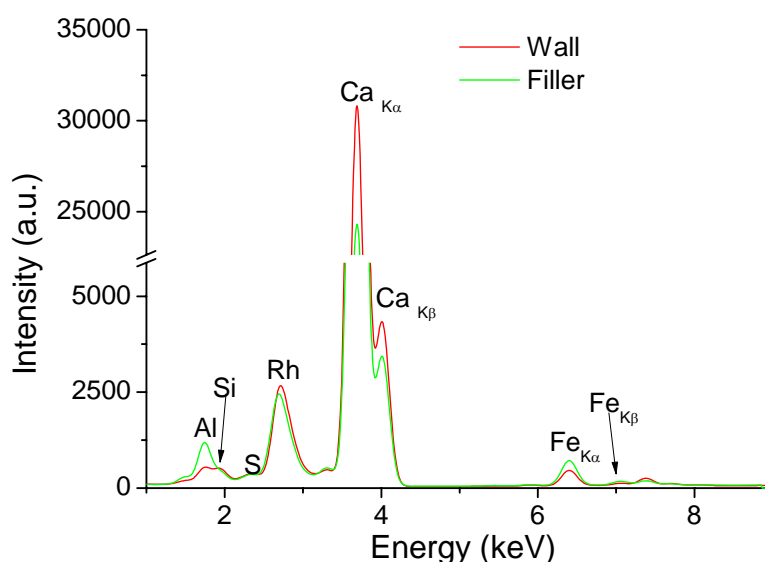


Figure 1. EDXRF analyses of the two samples.

WDS spectrometer attached to SEM equipment allows qualitative and quantitative analysis both of chalk sample and of restoration mortar, Figure 2. There are visible the difference between both samples and the changes in the Al/Si ratio, which is responsible for thaumasite and ettringite identification, too.

The X-ray diffraction patterns (figure 3) reveals that the mineralogical composition of the two samples is dominated by calcite (CC) and, in lesser extension, quartz (Q). A possible explanation for the differences observed by EDXRF and ICP-AES is the presence of traces of ettringite (E) and thaumasite (T) in the wall filler sample, concomitant with a decrease of calcite peaks. Thaumasite is a phase newly recognised in some sulphate-attacked building constructions. XRD giving direct qualitative evidence is generally accepted.

Thaumasite, $[\text{Ca}_3\text{Si}(\text{OH})_6 \cdot 12\text{H}_2\text{O}](\text{SO}_4)(\text{CO}_3)$ or $\text{CaSiO}_3 \cdot \text{CaCO}_3 \cdot \text{CaSO}_4 \cdot 15\text{H}_2\text{O}$, or $\text{Ca}_6[\text{Si}(\text{OH})_6 \cdot 12\text{H}_2\text{O}]_2(\text{SO}_4)_2(\text{CO}_3)_2$, is formed from external sulfate attack of cement concrete at low temperatures [11]. Its crystal structure is most unusual in that it contains silicon atoms that are surrounded by an octahedron of $\text{OH}^\#$ ions. This structure is closely related to that of ettringite, $\text{Ca}_6[\text{Al}(\text{OH})_6 \cdot 12\text{H}_2\text{O}]_2(\text{SO}_4)_3(\text{H}_2\text{O})_2$, and the two minerals form a series of solid solutions. Thaumasite tends to form at low temperatures ($4^\circ\text{C} - 10^\circ\text{C}$), in the presence of water. The presence of sulfate induces the formation of ettringite that uses aluminium provided by the cement. In the presence of sulfate and carbonate, thaumasite can continue to form until the calcium silicate hydrate is completely

decomposed. Sulfate can be supplied from the chalk damaged surfaces, and carbonate can be supplied from atmospheric CO₂ or from limestone present in the concrete or mortar.

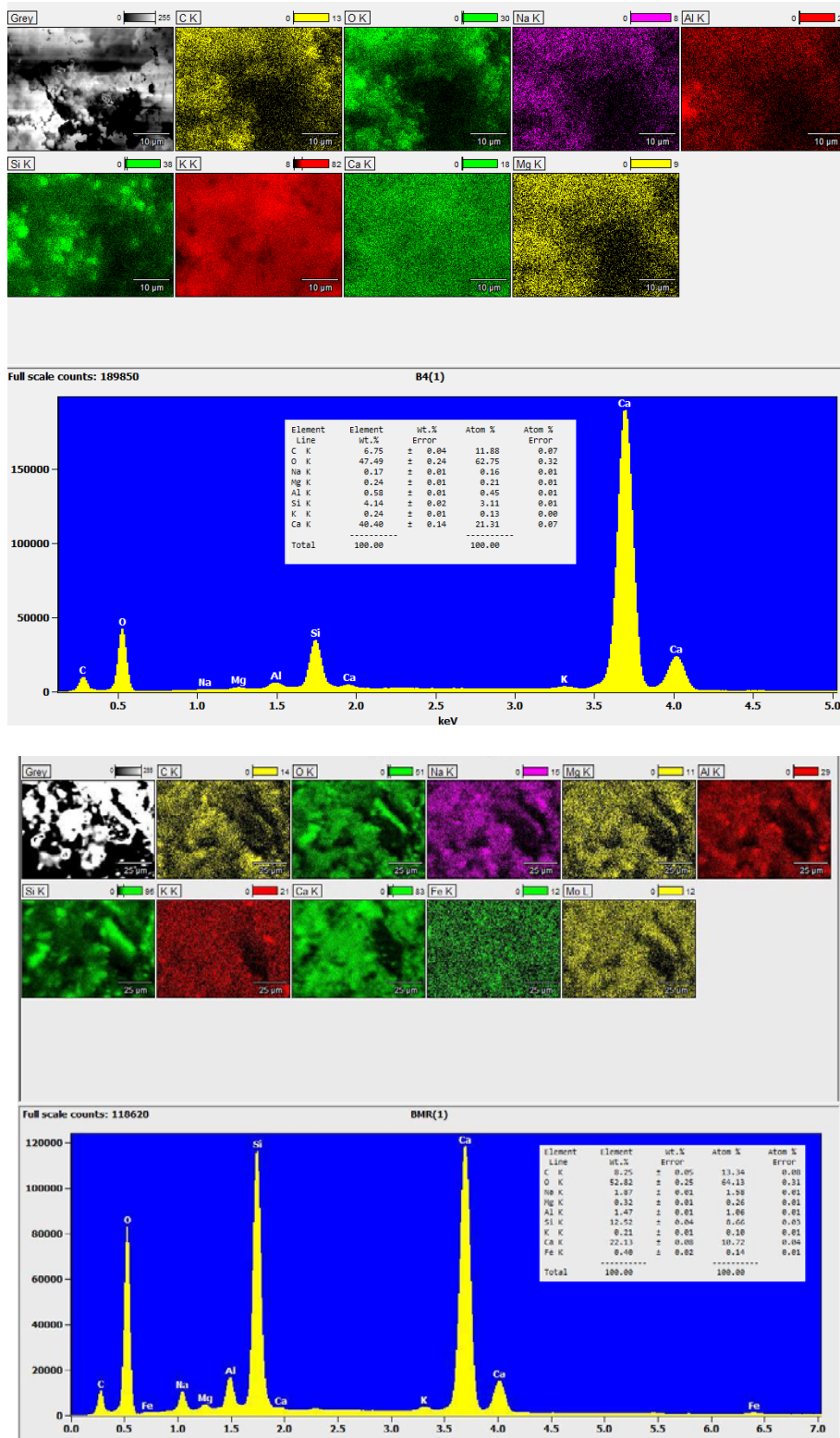


Figure 2. EDS results for chalk sample (up) and mortar sample (down).

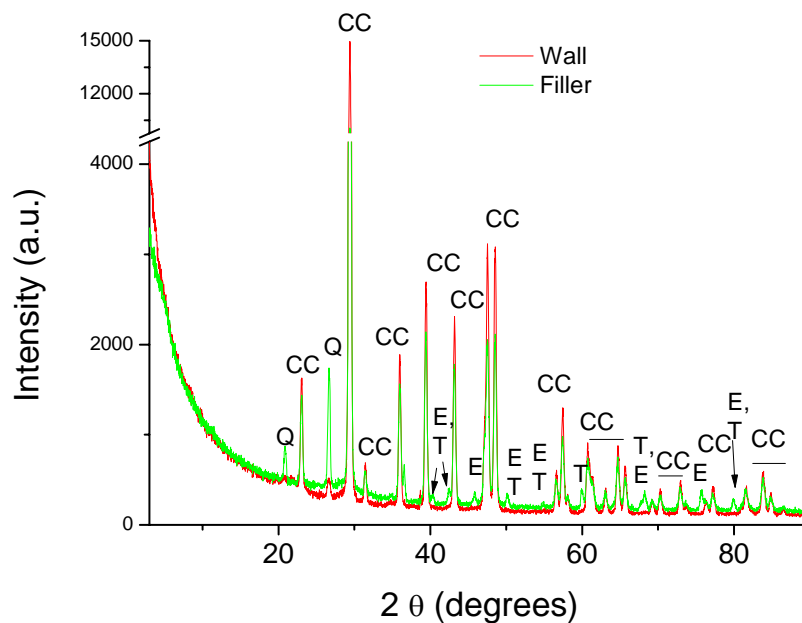


Figure 3. The XRD diagrams for chalk sample and mortar sample used for restoration.

The sulphate determination for chalk and mortar samples showed us higher concentration in mortar than in chalk sample, as follows: 0.87 % in chalk and 1.275 % in mortar. Both samples are affected by sulphate but in mortar the concentration is higher, this mortar becoming a dangerous damage factor for chalk.

By degradation, on the chalk surface no visible evidence could occurs, except effluorescence and small cracks, but on mortar large brown area could be observed most probably due to pyrite formation during degradation. Also, large smoothy deposits are present, with different structure, easy recognizable as thaumasite and probably ettringite, figure 4.



Figure 4.

The optical microscopy of chalk sample

The optical microscopy of restoration mortar

The chalk was found to be extensively deteriorated in both out-door and indoor environments in the studied historical monument, showing flaking, subflorescence, efflorescences, crumbling and black and white crusts as a result of the deterioration phenomena [12]. The infrared spectroscopic analysis carried out on the sample prelevated from Basarabi Church allowed the identification of the following products, as follows (figure 6):

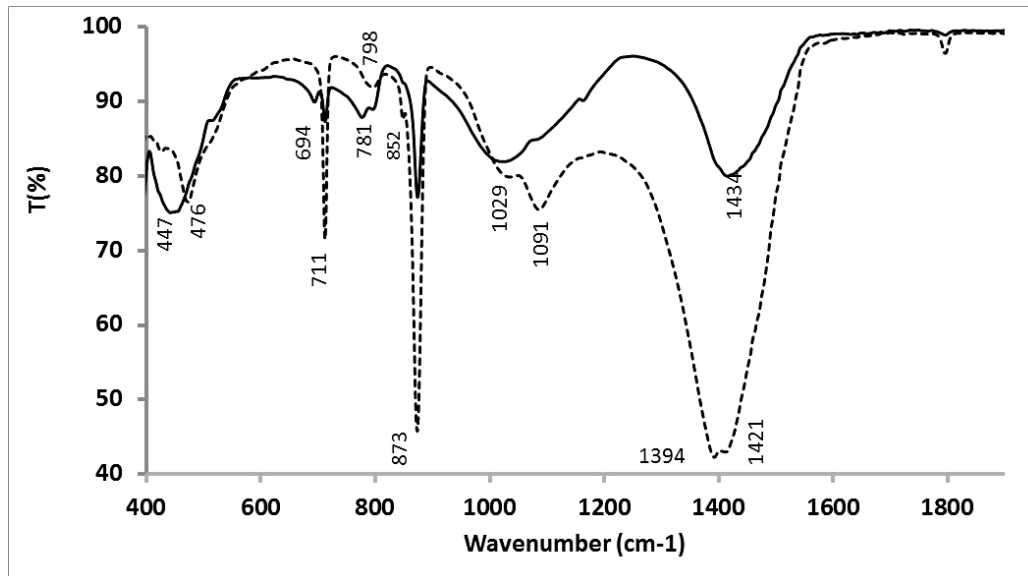


Figure 5. The FTIR spectra of chalk sample (---) and restoration mortar sample (___).

The spectrum shows specific bands for CO_3^{2-} stretching at 1409-1426, 873 SO_4^{2-} stretching at 1109 and 1029 cm^{-1} , band for Al-OH at 873 cm^{-1} , SiO₆ stretching at 798 and 476 cm^{-1} , Ca-OH bending at 611 cm^{-1} . These results are in good agreement with Perkins [13], Alvarez-Ayuso et al. [14], Myneni et al. [15] and Ciliberto et al. [16].

Also, Raman spectrum of the same sample (Fig. 6) displays characteristic bands of calcium carbonate that correspond to the vibration modes of the free CO_3^{2-} ion, located at approximately 1078 cm^{-1} , recognized as the strongest feature in this spectrum [16, 17]. *Thaumasite* has three major peaks at 658, 990, 1076 cm^{-1} and three minor peaks at 417, 453, 479 cm^{-1} . *Ettringite* has major peaks at 990, 1088 cm^{-1} .

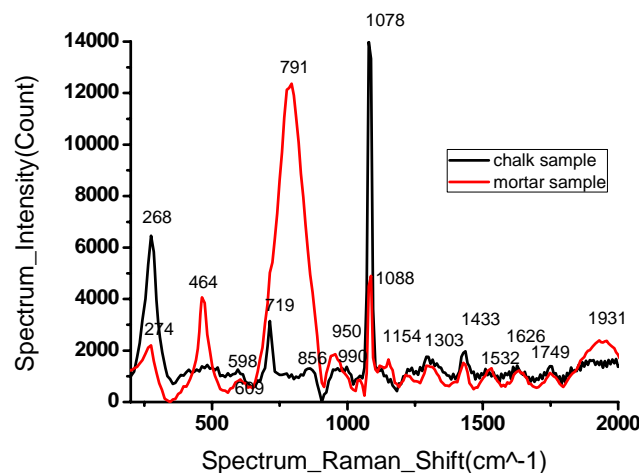


Figure 6. The Raman spectra of chalk (black) and restoration mortar (red line) samples.

Raman bands and assignments of ettringite are: 988 cm^{-1} (ν_1 symmetric stretching of (SO_4)), 448 cm^{-1} (ν_2 symmetric bending of (SO_4)), 1119 cm^{-1} (ν_3 asymmetric stretching of (SO_4)), 612 cm^{-1} (ν_4 asymmetric bending of (SO_4)), 547 cm^{-1} (Al-OH stretching) in very good agreement with other literature data [18]. It is important to mention that the above Raman frequencies are not of gypsum ($1009, 414, 493, 1136, 618, 670\text{ cm}^{-1}$). The presence of thaumasite and ettringite could be observed by SEM microscopy, these forms having shape of plaques (thaumasite-left image) and with some fluorish decorations (in mortar) for ettringite (right image), figure 7.

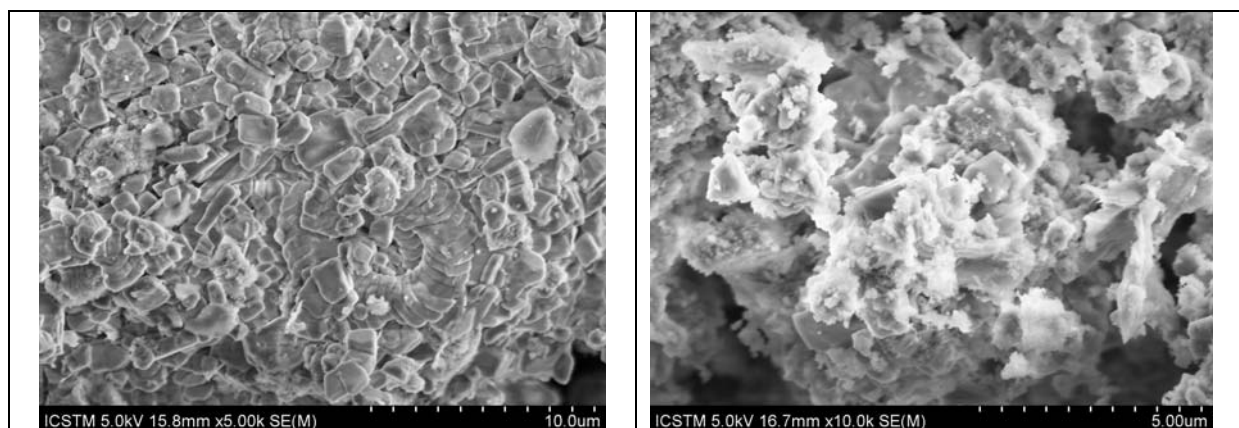


Figure 7. SEM images for chalk (left image) and restoration mortar (right image).

4. Conclusions

Cement-based materials exposed to sulfate present in the chalk stone - gypsum ($\text{CaSO}_4 \cdot 2\text{H}_2\text{O}$), can induce signs of deterioration, due to ettringite ($[\text{Ca}_3\text{Al}(\text{OH})_6 \cdot 12\text{H}_2\text{O}]_2 \cdot (\text{SO}_4)_3 \cdot 2\text{H}_2\text{O}$) or thaumasite ($\text{Ca}_3[\text{Si}(\text{OH})_6 \cdot 12\text{H}_2\text{O}] \cdot (\text{CO}_3) \cdot \text{SO}_4$) formation. These phases contribute to strain within the material, inducing severe degradation. Several combined techniques (XRD, EDXRF, ICP-AES, SEM, EDS, sulphates content, FT-IR and Raman) were carried out to put into evidence the effects of them on the building walls.

5. Acknowledgements

This paper has been prepared with the financial support of the projects PN II 261/2014 and PNII 222/2012.

References

- [1] P. Ferreira Pinto and J. Delgado Rodrigues, 2008 *J. Cult. Herit.*, 9, pp. 38.
- [2] A. E. Charola and R. Ware, 2002 Acid deposition and the deterioration of stone: a brief review of a broad topic, In: (eds) S. Siegesmund, T. Weiss and A. Vollbrecht, *Natural stone, weathering phenomena, conservation strategies and case studies* (Geological Society) Special Publication 205, pp. 393-406.
- [3] G. A. Pope, J. M. Stavash and J. C. Walker, 2002 Correlation of acid wet deposition with trends in stone deterioration at the local scale, R. Prikryl and H. A. Viles *Understanding and managing of stone decay ed*, pp. 297-316.
- [4] E. Doehne, 2002 Salt weathering: a selective review, (eds) S. Siegesmund, T. Weiss and A. Vollbrecht, *Natural stone, weathering phenomena, conservation strategies and case studies* (Geological Society) Special Publication 205, pp. 51-64.
- [5] J. Ondrasina, D. Kirchner and S. Siegesmund, 2002 Freeze - thaw cycles and their influence on marble deterioration: a long - term experiment, (eds) S. Siegesmund, T. Weiss and A. Vollbrecht, *Natural stone, weathering phenomena, conservation strategies and case studies* (Geological Society) Special Publication, 205, pp. 9-18.

- [6] T. Yates, 2003 Mechanism of air pollution damage to bricks, concrete and mortar, ed P. Brimblecombe, *The Effects of Air Pollution on the Built Environment*, pp. 107-122.
- [7] E. F. Irassar, V. L. Bonavetti, M. A. Trezza and M. A. González, 2005 *Cement and Concrete Composites*, 27(1), pp. 77.
- [8] M. Collepardi, 2003 *Cem. Conc. Comp.*, 25, pp. 401.
- [9] G. Cultrone, E. Sebastián and M. Ortega Huertas, 2005 *Cement and Concrete Research*, 35, pp. 2278.
- [10] R. M. Ion, D. Turcanu-Carutiu, R. C. Fierascu, I. Fierascu, I. R. Bunghez, M. L. Ion, S. Teodorescu, G. Vasilievici and V. Raditoiu, 2015 *Applied Surface Science*, 358B, pp. 612-618.
- [11] V. Gosselin, A. Verges-Belmin, V. Royer and G. Martinet, 2009 *Materials and Structures*, 42, pp. 749.
- [12] R. M. Ion, 2013 *Journal of Optoelectronics and Advanced Materials*, 15, pp. 888.
- [13] R. B. Perkins and C. D. Palmer, 1999 *Geochim. Cosmochim. Acta*, 63, pp. 1969.
- [14] E. Alvarez-Ayuso and H. W. Nugteren, 2005 *Water Res.*, 39, pp. 65.
- [15] S. C. B. Myneni, S. J. Traina, G. A. Waychunas and T. J. Logan, 1998 *Geochim. Cosmochim. Acta*, 62, pp. 3499.
- [16] E. Ciliberto, S. Ioppolo and F. Manuella, 2008 *J. Cult. Herit.*, 9, pp. 30.
- [17] Y. Yue, Y. Bai, P. A. Muhammed Basheer, J. J. Boland and J. J. Wang, 2013 *Optical Engineering*, 52(10), pp. 104107.
- [18] S. Kramar, M. Urosevic, H. Pristacz and H. Mirtic, 2010 *J. Raman Spectrosc.*, 11, pp. 1441.